

Reversible tuning of the surface state in a psuedo-binary $\text{Bi}_2(\text{Te-Se})_3$ topological insulator

Rui Jiang,^{1,2} Lin-Lin Wang,¹ Mianliang Huang,³ R. S. Dhaka,¹
Duane D. Johnson,¹ Thomas A. Lograsso,¹ and Adam Kaminski^{1,2,*}

¹*Division of Materials Science and Engineering, Ames Laboratory, Ames, IA 50011, USA*

²*Department of Physics and Astronomy, Iowa State University, Ames, IA 50011, USA*

³*Materials and Metallurgical Engineering Department,
South Dakota School of Mines, Rapid City, SD 57701*

We use angle-resolved photoemission spectroscopy to study non-trivial surface state in psuedo-binary $\text{Bi}_2\text{Se}_{0.6}\text{Te}_{2.3}$ topological insulator. We show that unlike previously studied binaries, this is an intrinsic topological insulator with conduction bulk band residing well above the chemical potential. Our data indicates that under good vacuum condition there are no significant aging effects for more then two weeks after cleaving. We also demonstrate that shift of the Kramers point at low temperature is caused by UV assisted absorption of molecular hydrogen. Our findings pave the way for applications of these materials in devices and present an easy scheme to tune their properties.

PACS numbers: 73.20.-r, 73.21.Fg, 79.60.Bm, 85.75.-d, 71.20.-b, 71.10.Pm, 73.20.At, 73.22.Gk

The prediction and subsequent discovery of surface state with nontrivial spin structure in topological insulators[1, 2] holds great promise to revolutionize spintronics and quantum computing. Such surface state has very unique properties as each electronic state in the momentum space is occupied by a single electron, unlike in traditional metals where two electrons with opposite spin reside at each momentum point. This leads to unusual spin structure at the chemical potential, where electrons at opposite momentum have also opposite spin. This obviously causes strong suppression of backscattering.

While several studies employing STM and ARPES techniques indeed show that electrons are immune to back scattering and nonmagnetic impurities[3, 4], the magnetic impurities, which break time reversal symmetry, can create additional surface states with odd number of Dirac fermions[5] and form a gap at Kramers point[7]. Other studies of effects of magnetic and nonmagnetic impurities on scattering rate[8] revealed that there is little difference between those two kinds of impurities.

The nontrivial surface state can surprisingly survive exposure to atmospheric pressure[11]. However, the electronic properties of topological insulator were shown to change significantly in vacuum with time[6, 9–11] with typical timescale of hours or even minutes after cleaving and usually results in formation of 2D electron gas. The delicate nature of the non-trivial surface state presents therefore series of challenges such as long-term stability and tunability before it can be utilized in a new class of devices. Beside most popular topological insulators Bi_2Se_3 and Bi_2Te_3 , the recently grown $\text{Bi}_2(\text{Te-Se})_3$ materials shows surprisingly large bulk resistivity[12] and low carrier concentration[13]. By doping Sb into this material, the Dirac cone can be tuned from n-type to p-type topological insulator[14].

In this Letter we demonstrate that under good vacuum

condition the electronic structure of the surface state in $\text{Bi}_2\text{Se}_{2x}\text{Te}_{2-2x}$ remains unchanged over a period of two weeks even after temperature cycling. We also show that this material is a “true” topological insulator, with bulk conduction band located well above the chemical potential and its electronic properties can be reversibly tuned by UV-assisted absorption of atomic hydrogen. This presents a simple way to tune the carrier concentration at the surface by adjusting device temperature in a low-pressure hydrogen atmosphere.

Single crystals were grown using proper ratio of high purity metals of bismuth (99.999 %), selenium (99.999%) and tellurium (99.999%) that were sealed in a quartz tube and melted into an ingot in an induction furnace to homogenize the composition. The ingot was then sealed in a quartz tube with a larger diameter and loaded into a Bridgman furnace. A crystal was grown by withdrawing the quartz tube at 1 mm/hr after being heated to 800°C. Chemistry of the sample was determined using electron probe micro-analysis (EPMA).

ARPES data was acquired using a laboratory-based system consisting of a Scienta SES2002 electron analyzer and GammaData Helium UV lamp. Samples were cleaved in-situ at room temperature with base pressure in the vacuum system at 5×10^{-11} Tr. All data were acquired using the HeI line with a photon energy of 21.2 eV. The angular resolution was 0.13° along and $\sim 0.5^\circ$ perpendicular to the direction of the analyzer slits. The energy resolution was set at ~ 6 meV. Custom designed refocusing optics enabled us to accumulate high statistics spectra in a short time to study sample aging effects. The results were reproduced on several samples and temperature cycling.

All DFT calculations have been done using VASP[19] on the (1×1) surface unit cell for $\text{Bi}_2\text{Te}_3(0001)$ with a slab of five atomic layers and 12 Å of vacuum. The bottom

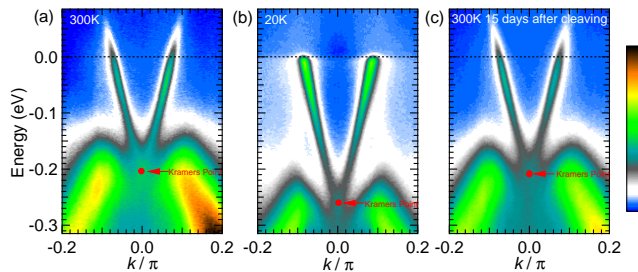


FIG. 1. Long term stability of the Dirac cone and temperature-induced changes in $\text{Bi}_2\text{Se}_{0.6}\text{Te}_{2.3}$. (a) Intensity plot along high-symmetry direction at 300K shortly after cleaving. (b) The data from the same cleave after cooling to 20K. The band moves to higher binding energy caused by electron doping. (c) The data from the same cleave as in (a) and (b) at 300 K after 15 days of continuous measurement and temperature cycling, also showing that the carrier concentration and band position is the same as in freshly cleaved sample.

two layers are fixed at bulk positions and the top three layers are free to relax until the absolute magnitude of force on each atom is reduced below $0.02 \text{ eV}/\text{\AA}$. A k -point mesh of $10 \times 10 \times 1$ with a Gaussian smearing of 0.05 eV and a kinetic energy cutoff of 300 eV were used.

In Figure 1, we examine the temperature dependence and stability of surface band in $\text{Bi}_2\text{Se}_{0.6}\text{Te}_{2.3}$ sample. Intensity plots show almost linear dispersion of the surface band and the absence of conduction bulk band at 300 K and 20 K. The Kramers point, i. e. the apex of Dirac cone, is below Fermi surface, which indicates a n-type topological insulator. After cooling to 20 K (panel b) the band moves to higher binding energy. This behavior was previously attributed to phonon effects [15] or photovoltaic effect [16]. Remarkably, after the sample was warmed up back to 300 K, the band structure recovers to its original state even though its surface was kept for 15 days in vacuum and exposed to UV and extensive temperature cycling (panel c).

We now focus on the cause of the changes in the band structure at low temperatures. In a fresh cleaved sample, the energy of Kramers point is -0.22 eV at 300 K, as shown in Figure 1a. We performed large number of consecutive measurements for each of the sample temperatures, with results shown in Figure 2. In panels a-d, we plot the Angle Resolved Photoemission Spectroscopy (ARPES) intensity at various temperatures and exposure times. After the sample was kept at 20 K for 90 hours we can observe the bulk conduction band, which for a clean surface, demonstrates that the chemical potential is located within the bulk band gap. In panel e, we show the evolution of the binding energy of the Kramers point with time and temperature. Each data point represents separate measurement and arrows mark the increase in sample temperature. When sample was kept at 20 K, the

Kramers point moves to higher binding energies, consistent with electron doping of the surface state. The process is relatively slow, which excludes scenarios involving phonons [15] or photovoltaic effect [16]. The associated large time constant suggests chemical doping of the surface as the origin. We note that the changes significantly slow down with time, indicating saturation effects which are most likely caused by the reduction of the sticking coefficient with increased coverage. The reverse effect, with a similar time constant, occurs upon warming up. Here, we rapidly increase the sample temperature to values indicated by the arrows and continuously perform multiple consecutive measurements at each temperature. The carrier concentration decreases with increasing temperature. In each case, a saturation level is reached when the sample is kept at fixed temperature for sufficiently long time.

The most likely suspect for the change of carrier concentration is the absorption of hydrogen. Even in the best vacuum system made of stainless steel, hydrogen is omnipresent. Upon cooling, it can condense onto the surface and donate electrons to the surface state. The binding energy of molecular hydrogen is quite low ($\sim 50 \text{ meV}$). It is possible, however, that UV light used for ARPES is causing its dissociation at the surface to atomic hydrogen that has a much larger binding energy. To validate our assertion about the origin of the shift, we dosed small amount of hydrogen into our vacuum system with and without UV. The binding energy of the Kramers point during this process is shown in Figure 3. At the beginning of measurement, without additional hydrogen, the binding energy of the Kramers point increases as in previous case and shifts downward by about 70 meV . We inject hydrogen with UV light switched off for 10 seconds at 10^{-7} Torr at time marked by black arrow in Figure 3. We do not observe any significant change after injection. Then we inject the same amount of hydrogen in the presence of UV light. Under those conditions the band shifts in energy by 36 meV , as measured immediately after injection. We repeat this process two more times. The drop is obvious each time, but with decreasing magnitude, indicating saturation of hydrogen on the surface of sample.

To support our proposition that the origin of electron doping and downward shift of Dirac point is due to absorption of atomic H, we used density functional theory (DFT)[17, 18] to calculate the adsorption of H_2 and H on $\text{Bi}_2\text{Te}_3(0001)$ surface. Figure 4 shows the DFT adsorption energy of H_2 as a function of distance to the surface with different exchange-correlation functionals at the hcp site with an out-of-plane orientation for H_2 . The data clearly shows that the interaction between H_2 and $\text{Bi}_2\text{Te}_3(0001)$ surface is of van der Waals type. PW91[21] gives a very weak binding of -28 meV at 3.7 \AA and LDA[20] gives a stronger binding of -80 meV at 2.4 \AA , which is closer to -71 meV at 3.2 \AA from

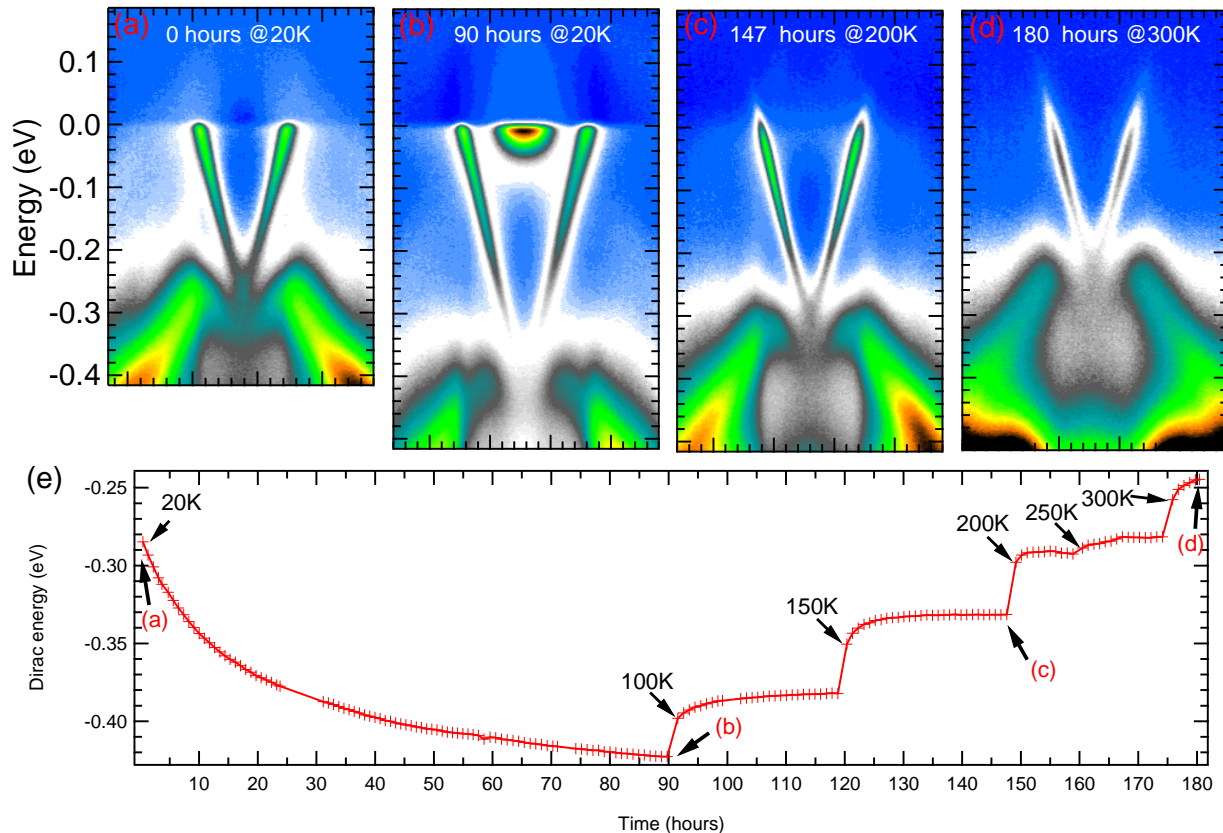


FIG. 2. Evolution of the band structure with time and temperature. (a)-(d) Intensity plot at temperatures and time indicated by arrows in panel (e). (e) Binding energy of the Kramers point as a function of time upon temperature cycling. Arrows mark the first measurement at a given temperature.

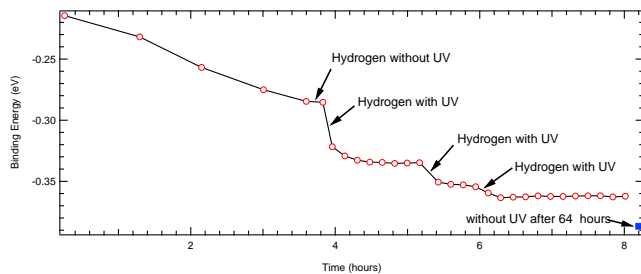


FIG. 3. The effects of hydrogen and UV Exposure. All measurement performed with sample at 20K. The black arrows indicate brief increase of hydrogen pressure (1×10^{-7} Torr for 10 sec.). The blue circle indicates binding energy of the Kramers point after 64 hours without UV light.

the more accurate description of the system by the van der Waals exchange-correlation functional[22]. Upon full relaxation, the bond length of the adsorbed H_2 is 0.77 Å, only slightly longer than the 0.75 Å of the free H_2 molecule. The relaxation of the surface atoms is negligible. The adsorption energy at the three adsorption (fcc, BRIDGE (brg) and top) sites is 5, 11 and 36 meV higher

than the hcp site, respectively. The difference in adsorption energy on the same site with different orientations of H_2 is less than 5 meV.

In contrast, the interaction between atomic H and $Bi_2Te_3(0001)$ surface is much stronger, with a binding energy of -1.41 eV at the brg site (in reference to a free atomic H), followed by -1.08 , -0.99 and -0.92 eV at the top, fcc and hcp sites, respectively. The space among the surface atoms can accommodate atomic H very well, the adsorbed H is in a co-planar position to surface Te atoms at all sites, except the top site, giving a binding distance of 1.73 Å. Although the adsorption energy in reference to a free H_2 molecule is 1.02 eV, which means that H_2 does not dissociate on $Bi_2Te_3(0001)$ surface, the presence of UV light during ARPES measurement can produce atomic H, as confirmed experimentally. In supporting evidence, we also directly calculated the shift of Dirac point in the surface band with different H_2 coverage. The downward shift due to the weak H_2 -surface interaction is about 20 meV, too small compared to the shift of 100 meV observed in experiment.

We have carefully detailed that the topological insulator behavior of $Bi_2Se_{0.6}Te_{2.3}$ remains unchanged and/or

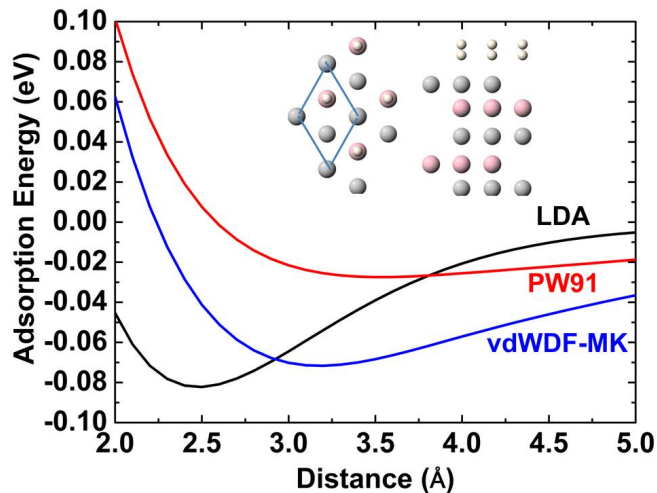


FIG. 4. Adsorption energy of H_2 on $Bi_2Te_3(0001)$ as a function of distance to the surface with LDA, PW91 and vdWDF-MK as exchange-correlation functional. The inset shows the top and side views of the relaxed structure. The (1×1) surface unit cell is highlighted in the top view. Red, gray and white spheres stand for Bi, Te and H, respectively.

controllable over extended periods under good vacuum conditions, distinct from commonly observed Rashba effects for example. We also showed that the Dirac cone electronic properties can be reversibly tuned by UV-assisted adsorption of atomic hydrogen, where DFT calculations confirm the assisted energetics and adsorption characteristics.

Research supported by the U.S. Department of Energy, Office of Basic Energy Sciences, Division of Materials Sciences and Engineering. Ames Laboratory is operated for

the U.S. Department of Energy by Iowa State University under Contract No. DE-AC02-07CH11358.

* kaminski@ameslab.gov

- [1] B. A. Bernevig, T. L. Hughes, & S.-C. Zhang, *Science* 314, 1757 (2006).
- [2] D. Hsieh *et al.*, *Nature* 452, 970 (2008).
- [3] P. Roushan *et al.*, *Nature* 460, 1106 (2009).
- [4] X.-L. Qi and S.-C. Zhang, *Rev. Mod. Phys.* 83, 1057 (2011).
- [5] L. A. Wray *et al.*, *Nature Phys.* 7, 32 (2010).
- [6] D. Hsieh *et al.*, *Phys. Rev. Lett.* 103, 146401 (2009).
- [7] Y. L. Chen *et al.*, *Science* 329, 659 (2010).
- [8] T. Valla *et al.*, *Phys. Rev. Lett.* 108, 117601 (2012).
- [9] Z. H. Zhu *et al.*, *Phys. Rev. Lett.* 107, 186405 (2011).
- [10] P. D. C. King *et al.*, *Phys. Rev. Lett.* 107, 096802 (2011).
- [11] C. Chen *et al.*, *Proc. Natl Acad Sci. USA* 109, 3694 (2012).
- [12] Zhi Ren *et al.*, *Phys. Rev. B* 82, 241306(R) (2010).
- [13] Shang Jia *et al.*, arxiv 1112, 1648v1 (2011).
- [14] T. Arakane *et al.*, *Nat. commun.* 3, 636 (2012).
- [15] Z. H. Pan *et al.*, arxiv 1109, 3638 (2011).
- [16] S. R. Park *et al.*, *New J. Phys.* 13, 013008 (2011).
- [17] P. Hohenberg and W. Kohn, *Phys. Rev.* 136, B864 (1964).
- [18] W. Kohn and L. J. Sham, *Phys. Rev.* 140, A1133 (1965).
- [19] G. Kresse and J. Furthmüller, *Phys. Rev. B* 54, 11169 (1996).
- [20] J. P. Perdew and A. Zunger, *Phys. Rev. B* 23, 5048 (1981).
- [21] J. P. Perdew and Y. Wang, *Phys. Rev. B* 45, 13244 (1992).
- [22] J. Klimes, D. R. Bowler and A. Michaelides, *Phys. Rev. B* 83, 195131 (2011).